Role of beam polarization in the determination of $WW\gamma$ and WWZ couplings from $e^+e^- \to W^+W^-$

V. V. Andreev*
International Centre for Theoretical Physics, Trieste, Italy

A. A. Pankov†
International Centre for Theoretical Physics, Trieste, Italy
and Istituto Nazionale di Fisica Nucleare, Sezione di Trieste, 34127 Trieste, Italy

N. Paver
Dipartimento di Fisica Teorica, Università di Trieste, 34100 Trieste, Italy
and Istituto Nazionale di Fisica Nucleare, Sezione di Trieste, 34127 Trieste, Italy

(Received 11 September 1995)

We evaluate the constraints on anomalous trilinear gauge-boson couplings that can be obtained from the study of electron-positron annihilation into W pairs at a facility with either the electron beam longitudinally polarized or both electron and positron beams transversely polarized. The energy ranges considered in the analysis are the ones relevant to the Next Linear Collider and to CERN LEP 200. We discuss the possibilities of a model-independent analysis of the general CP-conserving anomalous effective Lagrangian, as well as its restriction to some specific models with reduced number of independent couplings. The combination of observables with initial and final state polarizations allows us to separately constrain the different couplings and to improve the corresponding numerical bounds.

PACS number(s): 14.70.−e, 12.15.Ji, 12.60.−i, 13.10.+q

I. INTRODUCTION

The experimental confirmation of the standard model (SM) is presently limited to the sector of the interaction of fermions with vector bosons [1], where an impressive agreement is found. Another key ingredient of the SM, not tested yet, is the interaction in the gauge-boson sector, which follows from the non-Abelian structure of the electroweak symmetry and assures the renormalizability of the theory. Accordingly, in the physics program at planned high energy (and high luminosity) colliders, much emphasis is given to precise measurements of the $WW\gamma$ and WWZ couplings. Such measurements should eventually confirm the SM, or maybe discover ''anomalous'' values of these couplings indicating physics beyond the SM.

While experiments at low energy and precision measurements in e^+e^- annihilation at the Z^0 pole can provide *indirect* access to these constants [2–4], only high energy colliders, well above the threshold for W-pair production, will allow *direct* and unambiguous tests. In this regard, some limits are available from Fermilab Tevatron [5], and in the near future one can foresee experimental studies of boson self-couplings at the CERN e^+e^- collider LEP 200 [6–9], and to some extent at the DESY ep collider HERA [10]. A new stage in precision will be reached at the planned CERN Large Hadron Collider (LHC) [11,12] and at the e^+e^- linear colliders [13], taking advantage of the increased sensitivity to deviations from the SM allowed by the significantly higher c.m. energies of these machines.

A particularly sensitive process where to study the trilinear gauge boson couplings is the W-pair production [6]

$$e^+ + e^- \to W^+ + W^-. \tag{1}$$

In this process the enhanced sensitivity to anomalous values of those couplings reflects the partial compensation among the individual, $\sqrt{s}$-diverging contributions to the SM cross section ($\sqrt{s}$ is the c.m. energy), corresponding at the Born level to γ, ν, and Z exchange diagrams and their interferences. Instead, the SM couplings are such that the gauge cancellation exactly occurs in the asymptotic regime, and consequently the SM cross section has a decreasing behavior with $\sqrt{s}$ [14].

Considering the following modification of the γ- and Z-exchange amplitudes ($V=\gamma,Z$):

$$\mathscr{A}(V) \to \mathscr{A}(V) + \Delta\mathscr{A}(V) = (1+f_V)\mathscr{A}(V), \tag{2}$$

where f_V's linearly depend on the anomalous couplings, and introducing the relative deviation from the SM prediction for the cross section (either total, or differential, or integrated in some angular range):

$$\Delta \equiv \frac{\Delta\sigma}{\sigma_{\rm SM}} = \frac{\sigma_{\rm anom} - \sigma_{\rm SM}}{\sigma_{\rm SM}}, \tag{3}$$

one has

*Permanent address: Gomel State University, Gomel, 246699 Belarus.

†Permanent address: Gomel Polytechnical Institute, Gomel, 246746 Belarus. Electronic address: PANKOV@GPI.GOMEL.BY

 © 1996 The American Physical Society

$$\sigma_{\rm anom} \propto |\mathscr{A}_1(\nu)+(1+f_\gamma)\mathscr{A}(\gamma)+(1+f_Z)\mathscr{A}(Z)|^2 + |\mathscr{A}_2(\nu)|^2,$$

$$\sigma_{\rm SM} \propto |\mathscr{A}_1(\nu)+\mathscr{A}(\gamma)+\mathscr{A}(Z)|^2+|\mathscr{A}_2(\nu)|^2. \quad (4)$$

Here, taking into account the W^- (W^+) helicities τ (τ'), for later convenience the neutrino-exchange amplitude has been divided into the $|\tau-\tau'|\leqslant 1$ part $\mathscr{A}_1(\nu)$ plus the $|\tau-\tau'|=2$ part $\mathscr{A}_2(\nu)$. As evident in Eq. (4), the amplitude $\mathscr{A}_2(\nu)$ does not interfere with the others. To first order in f_V one obtains

$$\Delta=\Delta_\gamma+\Delta_Z, \quad (5)$$

where

$$\Delta_\gamma=f_\gamma(R_{\nu\gamma}+R_{Z\gamma}+2R_{\gamma\gamma}), \quad \Delta_Z=f_Z(R_{\gamma Z}+R_{\nu Z}+2R_{ZZ}), \quad (6)$$

and $(i,j=\gamma,\nu,Z)$

$$R_{ij}=\sigma_{ij}/\sigma_{\rm SM}, \quad \sigma_{\rm SM}\equiv\sigma(f_V=0)=\sum_{i,j}\sigma_{ij}. \quad (7)$$

In Eqs. (5)–(7), Δ's are determined by linear combinations of noncancelling individually divergent contributions, and will increase, basically like a power of s. In contrast, the SM cross section decreases at least as $1/s$. Thus, if we parametrize the sensitivity of process (1) to f_V by, e.g., the ratio $\mathscr{S}=\Delta/(\delta\sigma/\sigma)$, with $\delta\sigma/\sigma$ the statistical uncertainty experimentally attainable on the SM cross section, such a sensitivity is powerlike enhanced with increasing $\sqrt{s}$, even at fixed integrated luminosity, namely,[1] $\mathscr{S}\propto\sqrt{L_{\rm int}s}$.

As discussed in Ref. [15], a dramatic improvement in the sensitivity to anomalous values of $WW\gamma$ and WWZ vertices should be obtained if the initial electron beam were longitudinally polarized, and one could separately measure the cross sections for both $e^-_Le^+$ (σ^L) and $e^-_Re^+$ (σ^R) annihilation. In particular, although being suppressed by $\gamma-Z$ compensation and thus leading to lower statistics, σ^R has the advantage of being free of the neutrino-exchange contribution. In general, $\mathscr{A}_2(\nu)$ numerically dominates the SM $\sigma^{\rm unpol}$ and σ^L, and is not modified by anomalous trilinear couplings, so that it tends to diminish the sensitivity of these cross sections to such effects. Consequently, one can qualitatively expect σ^R to allow improved constraints even in the case of just one anomalous coupling taken as a free parameter.

In addition, for two (or more) free parameters, by themselves the cross sections σ^L and σ^R separately provide correlations among parameters rather than limits. In fact, from Eq. (4) and the approximate relation $\mathscr{A}(\gamma)\approx-\mathscr{A}^R(Z)\approx\mathscr{A}^L(Z)$ at $\sqrt{s}\gg M_Z$, the deviations of σ^L and σ^R from the SM are easily seen to bring information on the combinations

$$\Delta\sigma^L\propto f_\gamma+f_Z, \quad \Delta\sigma^R\propto f_\gamma-f_Z. \quad (8)$$

Due to $\sigma^L\gg\sigma^R$, also $\Delta\sigma^{\rm unpol}\propto f_\gamma+f_Z$. Clearly, the combination of σ^R and σ^L (or $\sigma^{\rm unpol}$) could be essential in order to significantly reduce the allowed region in the (f_γ,f_Z) plane, by the intersection of the "orthogonal" correlation areas provided by Eq. (8).

For realistic values of the electron longitudinal polarization, less than 100%, the determination of σ^R from the data could be contaminated by the uncertainty in the polarization itself, which allows the presence of some left-handed cross section. Due to $\sigma^L\gg\sigma^R$, such an uncertainty could induce a systematic error on σ^R larger than the statistical error for this cross section, and consequently the sensitivity would be diminished. However, as shown in Ref. [15], one can find "optimal" kinematical cuts to drastically reduce this effect.

In the general CP-conserving case, the anomalous effective Lagrangian for trilinear gauge boson couplings depends on five constants, which are difficult to disentangle from each other by using just the unpolarized cross section, not only due to the large number of parameters, but also due to possible accidental cancellations which might reduce the sensitivity of this observable. To separate the coupling constants, and constrain their values in a model-independent way, measurements of the cross sections for polarized final W's and both initial longitudinal polarizations should be combined.

In this paper we will present an estimate, along the lines exposed above, of the bounds on the anomalous three-boson coupling constants that can be obtained from the analysis of the process $e^+e^-\to W^+W^-$ based on the combination of polarized cross sections, at the reference energy of the planned e^+e^- linear colliders, namely 0.5 up to 1 TeV, with polarized electron beams and assuming that also W^+W^- polarization will be measured. A general discussion of the prospects and feasibility of measuring polarization effects in W-pair production can be found, e.g., in Refs. [8,17,18].

Also, we study the region around $\sqrt{s}=200$ GeV appropriate to LEP 200, since this machine will be operational in a relatively near future. Here, initial longitudinal polarization will not be available so that only unpolarized or transverse beam polarization will exist. The latter is an attractive option at e^+e^- storage rings such as LEP 200 [19,20], where electron and positron spins naturally align in opposite directions in the magnetic field of the accelerator. The transverse polarization could be exploited to perform the model-independent analysis, assuming the possibility of measuring final W^+W^- polarizations also in this case. In fact, for the "transverse" azimuthal asymmetry A_T (precisely defined in the sequel), one has $A_T\propto\mathscr{A}^L\mathscr{A}^R$ with $\mathscr{A}^L=\mathscr{A}(\nu)+\mathscr{A}(\gamma)+\mathscr{A}^L(Z)$ and $\mathscr{A}^R=\mathscr{A}(\gamma)+\mathscr{A}^R(Z)$ and, due to $\mathscr{A}^L\gg\mathscr{A}^R$, the deviation from the SM model is $\Delta A_T\propto f_\gamma-f_Z$. Consequently, to obtain the allowed region in the (f_γ,f_Z) plane, in this case A_T plays the same role as σ^R in the previous example in Eq. (8).

Specifically, in Sec. II we will introduce the standard parametrization of the $WW\gamma$ and WWZ vertices and will briefly review current and expected bounds on these parameters from forthcoming experiments. In Sec. III we introduce the helicity amplitudes and the corresponding observables relevant to our analysis and in Sec. IV we present the resulting constraints (model-independent as well as model-dependent ones) on the anomalous couplings from future

[1]This behavior of the sensitivity of process (1) also applies to other nonstandard effects, such as, e.g., Z-Z' mixing [15] and lepton mixing [16].

e^+e^- linear colliders. Section V is devoted to a similar analysis at the energy of LEP 200 and, finally, Sec. VI contains some concluding remarks. Formulas relevant to the cross sections needed for our numerical analysis are collected in the Appendix.

II. TRILINEAR GAUGE-BOSON VERTICES

We limit to the C- and P-invariant parts of the WWV interaction, which in general can be represented by the effective Lagrangian with five independent couplings [21]:

$$\mathscr{L}_{\rm eff}=-ie[A_\mu(W^{-\mu\nu}W^+_\nu-W^{+\mu\nu}W^-_\nu)+F_{\mu\nu}W^{+\mu}W^{-\nu}]-iex_\gamma F_{\mu\nu}W^{+\mu}W^{-\nu}-ie(\cot\theta_W+\delta_Z)[Z_\mu(W^{-\mu\nu}W^+_\nu-W^{+\mu\nu}W^-_\nu)$$
$$+Z_{\mu\nu}W^{+\mu}W^{-\nu}]-iex_ZZ_{\mu\nu}W^{+\mu}W^{-\nu}+ie\frac{y_\gamma}{M_W^2}F^{\nu\lambda}W^-_{\lambda\mu}W^{+\mu}_\nu+ie\frac{y_Z}{M_W^2}Z^{\nu\lambda}W^-_{\lambda\mu}W^{+\mu}_\nu, \tag{9}$$

where $W^\pm_{\mu\nu}=\partial_\mu W^\pm_\nu-\partial_\nu W^\pm_\mu$ and $Z_{\mu\nu}=\partial_\mu Z_\nu-\partial_\nu Z_\mu$. In Eq. (9), $e=\sqrt{4\pi\alpha_{em}}$ and θ_W is the electroweak angle. The relation of the above constants to those more directly connected with W static properties is

$$x_\gamma\equiv\Delta k_\gamma=k_\gamma-1,\quad y_\gamma\equiv\lambda_\gamma,\quad \delta_Z\equiv g_Z-\cot\theta_W,$$
$$x_Z\equiv\Delta k_Z(\cot\theta_W+\delta_Z)=(k_Z-1)g_Z,$$
$$y_Z\equiv\lambda_Z\cot\theta_W. \tag{10}$$

With μ_W and Q_W the W magnetic and quadrupole electric moments, respectively,

$$\mu_W=\frac{e}{2M_W}(1+k_\gamma+\lambda_\gamma),\quad Q_W=-\frac{e}{M_W^2}(k_\gamma-\lambda_\gamma), \tag{11}$$

and a similar interpretation holds for the WWZ couplings.

At the tree level, the SM values of these couplings are

$$\delta_Z=x_\gamma=x_Z=y_\gamma=y_Z=0. \tag{12}$$

In the SM, the natural size of Δk_γ and λ_γ is $\alpha_{\rm em}/\pi\sim10^{-3}$ [22]. In extensions of the SM such as those containing extra Higgs doublets, extra heavy fermions [23], or supersymmetric extensions [24,25], the deviations from the tree-level SM values tend to be of the same order of magnitude as these one-loop corrections.

Briefly summarizing the present information and the future perspectives concerning the anomalous couplings, *indirect* constraints on $WW\gamma$ and WWZ vertices have been obtained by comparing low energy data ($\sqrt{s}<2M_W$) with SM predictions for observables that can involve such vertices at the loop level [3,26]. These limits are derived from a global analysis of the data varying one parameter at a time and keeping the remaining ones fixed at the SM values, and are relatively weak with respect to the size of the SM corrections: $|\Delta k_\gamma|\leqslant0.12$, $|\Delta k_Z|\leqslant0.08$, $|\lambda_\gamma|\leqslant0.07$, and $|\lambda_Z|\leqslant0.09$ at 95% CL [26].

Direct tests of trilinear gauge boson couplings at higher energies ($\sqrt{s}>2M_W$) have been attempted in $p\bar{p}\to W^\pm\gamma$, $W^\pm Z$, and W^+W^- at the Tevatron, still considering one constant at a time as a free parameter [5]. In this case, limits are of the order of unity, and therefore are not yet stringent enough to significantly test the SM. The expected sensitivities from future Tevatron experiments are $|\Delta k_\gamma|$, $|\lambda_\gamma|\sim0.1$ at $\int Ldt=1fb^{-1}$, and in the longer term the hadron collider LHC would improve the Tevatron bounds for $\Delta k_{\gamma,Z}$ and $\lambda_{\gamma,Z}$ to an accuracy in the range ~0.01–0.1, assuming an integrated luminosity of 100 fb^{-1} [12].

In the near perspective, some constraint on the $WW\gamma$ vertex to an accuracy of about ±0.5 should be obtainable at HERA from single W production [10].

Indeed, the test of the trilinear gauge boson couplings from the W pair production process (1) will be one of the major items in the forthcoming physics program at LEP 200 [6–9], where an accuracy of ~0.1 is expected from direct measurements of the cross section.

In the more distant future, the Next Linear e^+e^- Colliders (NLC's), with $\sqrt{s}\geqslant500$ GeV [21,27], will probably provide the best opportunities to analyze gauge boson couplings with significant accuracy from the $W^\pm$ pair production process (1), due to the really high sensitivity of this reaction at such energies, in particular if initial beam polarization will be available. Depending on the c.m. energy and the integrated luminosity, it should be possible to test those couplings *via* a model-independent analysis, and look for deviations from the SM with an accuracy up to some units $\times10^{-3}$.

In the next section, we present the helicity amplitudes and the polarized observables relevant to the analysis of process (1).

III. HELICITY AMPLITUDES AND POLARIZED CROSS SECTIONS

In Born approximation, process (1) is described by the ν, γ, and Z exchange amplitudes in Fig. 1. The differential

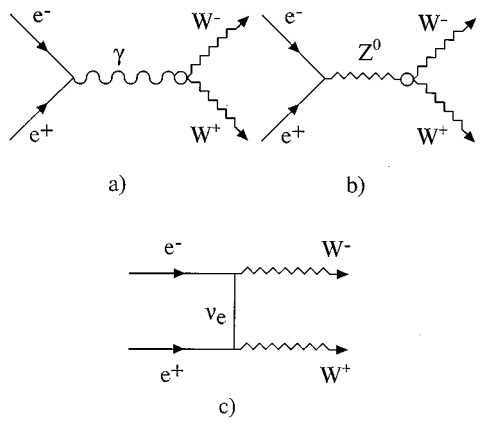

FIG. 1. The Feynman diagrams for the $e^+e^-\to W^+W^-$.

TABLE I. Helicity amplitudes for $e^+e^-\to W^+W^-$.

$e^+_{-\lambda}e^-_{\lambda}\to W^+_L W^-_L$	$\tau=\tau'=0$	
	$-\frac{e^2 S\lambda}{2}\sin\theta$	
$\frac{2\lambda-1}{4ts_W^2}$	$\frac{S}{2M_W^2}\left[\cos\theta-\beta_W\left(1+\frac{2M_W^2}{S}\right)\right]$	
$-\frac{2}{S}+\frac{2\cot\theta_W}{S-M_Z^2}(v-2a\lambda)$	$-\beta_W\left(1+\frac{S}{2M_W^2}\right)$	
$-\frac{x_\gamma}{S}+\frac{x_Z+\delta_Z(3-\beta_W^2)/2}{S-M_Z^2}(v-2a\lambda)$	$-\beta_W\frac{S}{M_W^2}$	
$e^+_{-\lambda}e^-_{\lambda}\to W^+_T W^-_T$	$\tau=\tau'=\pm1$	$\tau=-\tau'=\pm1$
	$-\frac{e^2 S\lambda}{2}\sin\theta$	$-\frac{e^2 S\lambda}{2}\sin\theta$
$\frac{2\lambda-1}{4ts_W^2}$	$\cos\theta-\beta_W$	$-\cos\theta-2\tau\lambda$
$-\frac{2}{S}+\frac{2\cot\theta_W}{S-M_Z^2}(v-2a\lambda)$	$-\beta_W$	0
$-\frac{y_\gamma}{S}+\frac{y_Z+\delta_Z(1-\beta_W^2)/2}{S-M_Z^2}(v-2a\lambda)$	$-\beta_W\frac{S}{M_W^2}$	0
$e^+_{-\lambda}e^-_{\lambda}\to W^+_T W^-_L$	$\tau=0,\ \tau'=\pm1$	$\tau=\pm1,\ \tau'=0$
	$-\frac{e^2 S\lambda}{2\sqrt{2}}(\tau'\cos\theta-2\lambda)$	$\frac{e^2 S\lambda}{2\sqrt{2}}(\tau\cos\theta+2\lambda)$
$\frac{2\lambda-1}{4tS_W^2}$	$\frac{\sqrt{S}}{2M_W}[\cos\theta(1+\beta_W^2)-2\beta_W]$	$\frac{\sqrt{S}}{2M_W}[\cos\theta(1+\beta_W^2)-2\beta_W]$
	$-\frac{2M_W}{\sqrt{S}}\frac{\tau'\sin^2\theta}{\tau'\cos\theta-2\lambda}$	$-\frac{2M_W}{\sqrt{S}}\frac{\tau\sin^2\theta}{\tau\cos\theta+2\lambda}$
$-\frac{2}{S}+\frac{2\cot\theta_W}{S-M_Z^2}(v-2a\lambda)$	$-\beta_W\frac{\sqrt{S}}{M_W}$	$-\beta_W\frac{\sqrt{S}}{M_W}$
$-\frac{x_\gamma+y_\gamma}{S}+\frac{x_Z+y_Z+2\delta_Z}{S-M_Z^2}(v-2a\lambda)$	$-\beta_W\frac{\sqrt{S}}{M_W}$	$-\beta_W\frac{\sqrt{S}}{M_W}$

cross section for initial e^+_λ, e^-_λ and final $W^+_{\tau'}, W^-_\tau$ states can be expressed as

$$\frac{d\sigma^{\lambda\lambda'}_{\tau\tau'}}{d\cos\theta}=\frac{|\vec{p}|}{4\pi s\sqrt{s}}|\mathscr{A}^{\lambda\lambda'}_{\tau\tau'}(s,\cos\theta)|^2. \tag{13}$$

In Eq. (13), $|\vec{p}|=\beta_W\sqrt{s}/2$, $\beta_W=\sqrt{1-4M_W^2/s}$, $\lambda=\pm1/2$ with $\lambda'=-\lambda$ represents the electron (positron) helicities, and $\tau(\tau')=\pm1,0$ are the W^- (W^+) helicities.

The helicity amplitudes $\mathscr{A}^{\lambda\lambda'}_{\tau\tau'}$ are listed in Table I, in a form convenient to our analysis [21]. The notation is such that $t=M_W^2-s(1-\beta_W\cos\theta)/2$, $v=(T_{3,e}-2Q_e s_W^2)/2s_W c_W$, and $a=T_{3,e}/2s_W c_W$, where t is the momentum transfer and v and a are, respectively, the SM vector and axial-vector couplings of electrons to the Z boson ($s_W=\sin\theta_W$, $c_W=\cos\theta_W$). The first column in Table I contains the relevant combinations of coupling constants and propagators, while the remaining two contain kinematical factors. In order to obtain the amplitude for definite electron helicity λ and $W^\mp$ helicities τ and τ', one has to sum the products of all the relevant entries in the first column times the corresponding kinematical factor in the same row times the common kinematical factor on top of the second (or of the third) column.

In a circular storage ring collider, such as LEP 200, transverse polarization of electron and positron beams can naturally occur. Thus, introducing for e^- and e^+ the magnitudes of longitudinal and transverse polarizations, P_L, P'_L and P_T, P'_T, the averaged square of the matrix element for arbitrarily polarized initial beams can be written as [19,20]

$$\overline{|\mathscr{A}|^2}=\frac{1}{4}\{(1-P_LP'_L)[|\mathscr{A}^+|^2+|\mathscr{A}^-|^2]+(P_L-P'_L)[|\mathscr{A}^+|^2-|\mathscr{A}^-|^2]+2P_TP'_T[\cos(2\phi_W)\mathrm{Re}(\mathscr{A}^+\mathscr{A}^-{}^*)-\sin(2\phi_W)\mathrm{Im}(\mathscr{A}^+\mathscr{A}^-{}^*)]\},\tag{14}$$

where ϕ_W is the azimuthal production angle of the W^- and $\mathscr{A}^{\pm}$ correspond to $\lambda=-\lambda'=\pm 1/2$ for arbitrary $W^{\mp}$ helicities τ,τ'.

Integrating over the angle ϕ_W, and assuming $P'_L=0$, the differential cross section reads

$$\frac{d\sigma}{d\cos\theta}=\frac{1}{4}\left[(1+P_L)\frac{d\sigma^+}{d\cos\theta}+(1-P_L)\frac{d\sigma^-}{d\cos\theta}\right],\tag{15}$$

where

$$\frac{d\sigma^{+,-}}{d\cos\theta}=\frac{|\vec{p}|}{4\pi s\sqrt{s}}|\mathscr{A}^{+,-}|^2.\tag{16}$$

In practice, the initial electron longitudinal polarization P_L will not be exactly equal to unity, so that the measured cross section will be a linear combination of σ^+ and σ^- as in Eq. (15), with $|P_L|<1$. In what follows, we shall refer to "right-handed" (σ^R) and "left-handed" (σ^L) cross sections the cases $P_L=0.9$ and $P_L=-0.9$, respectively. Such values of P_L seem to be obtainable at the NLC [28].

Concerning the possibility of exploiting transverse beam polarization, which will be taken into account for LEP 200 only, a suitable observable is the azimuthal asymmetry A_T, defined as

$$\frac{d(\sigma A_T)}{d\cos\theta}=2\int_0^{2\pi}\frac{d^2\sigma}{d\cos\theta\,d\phi_W}\cos(2\phi_W)d\phi_W=P_TP'_T\frac{|\vec{p}|}{4\pi s\sqrt{s}}\mathrm{Re}(\mathscr{A}^+\mathscr{A}^-{}^*).\tag{17}$$

In our numerical results we shall assume $P_T=P'_T=92.4\%$, which is the maximum attainable value.

IV. BOUNDS ON ANOMALOUS COUPLINGS FROM NLC

Present constraints on anomalous couplings are obtained by taking only one or two of them at a time as independent free parameters, and fixing the remaining ones at the SM values or, alternatively, by assuming specific models where the couplings are related to each other so that the number of degrees of freedom is reduced. Bounds derived in this way, although seemingly stringent, might not fully represent the real situation that can occur in general. Indeed, when allowing for more than one anomalous coupling, correlations among these parameters and/or accidental cancellations can possibly reduce the sensitivity, if a restricted set of observables, such as the unpolarized differential or the total cross section, is considered. To the purpose of making a significant test by disentangling the various couplings, it should be desirable to apply a model-independent analysis, where all trilinear gauge boson couplings of Eq. (9) are included and allowed to vary independently. In this regard, as we shall see below, polarization not only allows to disentangle the bounds for the different constants in a simple, analytic, way, but also leads to definite improvements in the accuracy of the constraints.

Using Table I one easily finds that, for specific initial and final state polarizations, the deviations from the SM of the γ and Z exchange amplitudes depend on the following combinations of anomalous couplings:

$$\Delta\mathscr{A}^a_{LL}(\gamma)\propto x_\gamma,\quad \Delta\mathscr{A}^a_{LL}(Z)\propto\left(x_Z+\delta_Z\frac{3-\beta_W^2}{2}\right)g_e^a,\tag{18}$$

$$\Delta\mathscr{A}^a_{TL}(\gamma)\propto x_\gamma+y_\gamma,\quad \Delta\mathscr{A}^a_{TL}(Z)\propto(x_Z+y_Z+2\delta_Z)g_e^a,\tag{19}$$

$$\Delta\mathscr{A}^a_{TT}(\gamma)\propto y_\gamma,\quad \Delta\mathscr{A}^a_{TT}(Z)\propto\left(y_Z+\delta_Z\frac{1-\beta_W^2}{2}\right)g_e^a.\tag{20}$$

In Eqs. (18)–(20) the lower indices LL, TL, and TT refer to the final W^-W^+ polarizations, and the upper index a indicates the initial e^- right-handed ($^+$) or left-handed ($^-$) polarizations, with $g_e^R=s_W/c_W$ and $g_e^L=g_e^R(1-1/2s_W^2)$ the corresponding electron couplings to the Z.

In order to assess the sensitivity of the different cross sections to the gauge-boson couplings we divide the experimentally significant range of the production angle $\cos\theta$ (which we take as $|\cos\theta|\leqslant 0.98$) into "bins," and define the χ^2 function:

$$\chi^2=\sum_i^{\text{bins}}\left[\frac{N_{\mathrm{SM}}(i)-N_{\mathrm{anom}}(i)}{\delta N_{\mathrm{SM}}(i)}\right]^2.\tag{21}$$

As it is conventional in this kind of analyses, the range of $\cos\theta$ is divided into 10 equal bins for the NLC and into 6 bins for the LEP 200 case. In Eq. (21), in a self-explaining notation $N(i)=L_{\mathrm{int}}\sigma_i\varepsilon_W$ is the expected number of events in the ith bin, with σ_i the corresponding cross section (either the SM or the anomalous one):

$$\sigma_i\equiv\sigma(z_i,z_{i+1})=\int_{z_i}^{z_{i+1}}\left(\frac{d\sigma}{dz}\right)dz,\tag{22}$$

where $z=\cos\theta$. For convenience, in the Appendix we give the explicit expressions for the polarized integrated cross sections $\sigma(z_i,z_{i+1})$ with nonzero anomalous gauge boson couplings. The parameter ε_W introduced above is the efficiency for W^+W^- reconstruction in the considered polarization state. We take the channel of lepton pairs ($e\nu+\mu\nu$) plus two hadronic jets, and correspondingly a reference value $\varepsilon_W\simeq 0.3$, [18,29–31] as obtained from the relevant branching ratios. The actual value of ε_W for polarized final states might be considerably smaller, depending on experimental details [18], but definite estimates are presently not available. As a compensation, for the luminosity L_{int}, which everywhere appears multiplied by ε_W, we make the rather conservative choice compared with recent findings [32]:

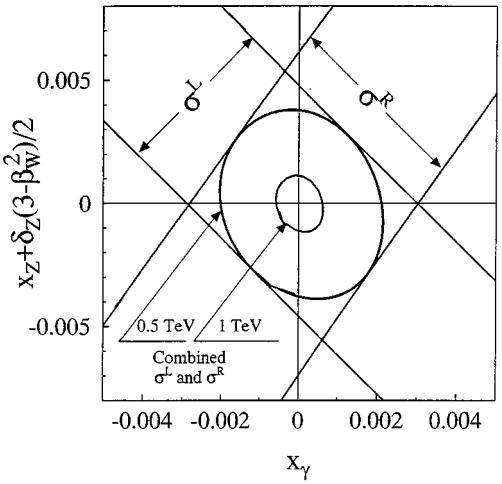

FIG. 2. Allowed domains (95% C.L.) for $[x_\gamma, x_Z+\delta_Z(3-\beta_W^2)/2]$ from $e^+e^-\to W_L^+W_L^-$ with longitudinally polarized electrons at $\sqrt{s}=0.5$ TeV and at $\sqrt{s}=1$ TeV, inputs as specified in the text.

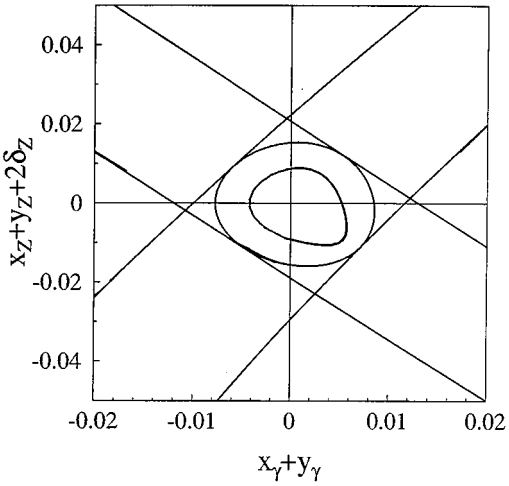

FIG. 3. Allowed domains (95% C.L.) for $(x_\gamma+y_\gamma, x_Z+y_Z+2\delta_Z)$ from $e^+e^-\to W_L^+W_T^-+W_T^+W_L^-$ with same inputs as in Fig. 2.

$$\int L\,dt=20\ \text{fb}^{-1}\quad(\text{NLC 500}),$$

$$\int L\,dt=50\ \text{fb}^{-1}\quad(\text{NLC 1000}). \tag{23}$$

Finally, in Eq. (21), the uncertainty on the number of events $\delta N_{\rm SM}(i)$ combines both statistical and systematic errors for the ith bin:

$$\delta N_{\rm SM}(i)=\sqrt{N_{\rm SM}(i)+[\delta_{\rm syst}N_{\rm SM}(i)]^2}, \tag{24}$$

and the systematic error will be taken as $\delta_{\rm syst}=2\%$.

As a criterion to derive allowed regions for the coupling constants, we will impose that $\chi^2\leqslant\chi^2_{\rm crit}$, where $\chi^2_{\rm crit}$ is a number that specifies a chosen confidence level and in principle can depend on the kind of analysis. Eqs. (18)–(20) show that each polarized cross section involves two well-defined combinations of anomalous couplings at a time, namely $[x_\gamma, x_Z+\delta_Z(3-\beta_W^2)/2]$, $(x_\gamma+y_\gamma, x_Z+y_Z+2\delta_Z)$, and $[y_\gamma, y_Z+\delta_Z(1-\beta_W^2)/2]$. Correspondingly, with two independent degrees of freedom, in each separate case bounds at the 95% C.L. are obtained by choosing[2] $\chi^2_{\rm crit}=6$ [33,34]. The same $\chi^2_{\rm crit}=6$ is taken in order to derive 95% C.L. bounds on the coupling constants from the combination of both initial longitudinal polarizations, $d\sigma^R/dz$ $(P_L=0.9)$ and $d\sigma^L/dz$ $(P_L=-0.9)$, for which the combined χ^2 function is defined as the sum $\chi^2=\chi^2_R+\chi^2_L$.

We start the presentation of our numerical results from the case of longitudinally polarized W's, $e^-e^+\to W_L^-W_L^+$, for both possibilities of electron beam longitudinal polarization. The resulting area allowed to the combinations of anomalous couplings in Eq. (18) at the 95% C.L. is depicted in Fig. 2, for both $\sqrt{s}=0.5$ and 1 TeV. Actually, as discussed in Ref. [35], one finds elliptical contours which would give four common intersections as allowed regions, three of them not containing the SM values. Obviously, we are concentrating here on the region surrounding zero values for anomalous couplings. This information is not yet sufficient to disentangle the individual couplings, since from Fig. 2 we simply find the pair of inequalities

$$-\alpha_1^{LL}<x_\gamma<\alpha_2^{LL}, \tag{25}$$

$$-\beta_1^{LL}<x_Z+\delta_Z\frac{3-\beta_W^2}{2}<\beta_2^{LL}, \tag{26}$$

so that only x_γ is separately constrained at this stage. Here, $\alpha_{1,2}^{LL}$ and $\beta_{1,2}^{LL}$ are the projections of the combined allowed area on the horizontal and vertical axes, respectively, and their values can be directly read from Fig. 2.

Turning to the other polarized cross sections, we repeat the same analysis there. From $e^+e^-\to W_T^+W_L^-+W_L^+W_T^-$ we

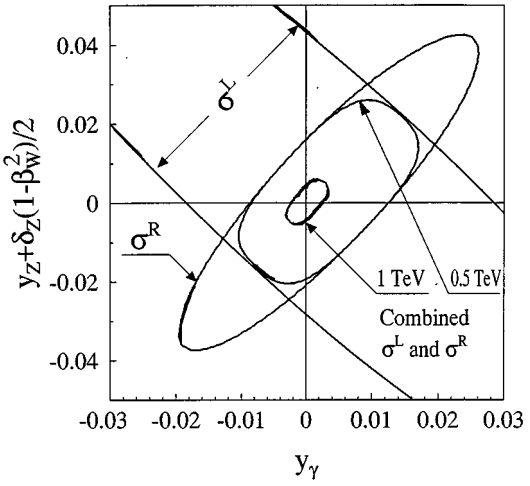

FIG. 4. Allowed domains (95% C.L.) for $[y_\gamma, y_Z+\delta_Z(1-\beta_W^2)/2]$ from $e^+e^-\to W_T^+W_T^-$ with same inputs as in Fig. 2.

[2]This should be compared with the case of only one free parameter, which occurs in various models, where $\chi^2_{\rm crit}=4$ should be taken to obtain the bounds at the same C.L.

TABLE II. Model-independent limits on the five CP-even nonstandard gauge boson couplings at the 95% C.L.

$\sqrt{s}$(TeV)	$x_\gamma(10^{-3})$	$y_\gamma(10^{-3})$	$\delta_Z(10^{-3})$	$x_Z(10^{-3})$	$y_Z(10^{-3})$
0.5	$-2.0-2.2$	$-11.0-10.6$	$-52-45$	$-51-59$	$-22-30$
1	$-0.6-0.6$	$-3.2-3.4$	$-19-16$	$-18-20$	$-5.7-6.2$

obtain the allowed region for the combinations of coupling constants in Eq. (19), depicted in Fig. 3. This leads to the following inequalities, analogous to Eqs. (25) and (26):

$$-\alpha_1^{TL}<x_\gamma+y_\gamma<\alpha_2^{TL}, \tag{27}$$

$$-\beta_1^{TL}<x_Z+y_Z+2\,\delta_Z<\beta_2^{TL}. \tag{28}$$

Finally, from $e^+e^-\to W_T^+W_T^-$ one obtains for the combinations of coupling constants in Eq. (20) the allowed regions depicted in Fig. 4, and the corresponding inequalities

$$-\alpha_1^{TT}<y_\gamma<\alpha_2^{TT}, \tag{29}$$

$$-\beta_1^{TT}<y_Z+\frac{1-\beta_W^2}{2}\delta_Z<\beta_2^{TT}. \tag{30}$$

One can notice that, with initial state polarization, the channel $e^+e^-\to W_T^+W_T^-$ can separately constrain y_γ. The limits in Fig. 4 are less restrictive compared to the previous cases, because they are determined by the larger width of the region allowed by the left-handed cross section, which is dominated by the $|\tau-\tau'|=2$ amplitude $\mathscr{A}_2(\nu)$ [see Eq. (4)] and therefore has a reduced sensitivity to anomalous couplings. Moreover, comparing Fig. 4 to Figs. 2 and 3, one can notice that the bound resulting from σ^R has now a quite different shape. This is the dramatic effect of the contamination of the right-handed cross section by the much bigger left-handed one for P_L not exactly equal to unity ($P_L=0.9$), as it can be seen from Eq. (15).

By combining Eqs. (26)–(30), one can very simply disentangle the bounds for δ_Z, x_Z, and y_Z:

$$-\frac{1}{\beta_W^2}B_2<\delta_Z<\frac{1}{\beta_W^2}B_1, \tag{31}$$

$$-\left(\beta_1^{LL}+\frac{3-\beta_W^2}{2\beta_W^2}B_1\right)<x_Z<\beta_2^{LL}+\frac{3-\beta_W^2}{2\beta_W^2}B_2, \tag{32}$$

$$-\left(\beta_1^{TT}+\frac{1-\beta_W^2}{2\beta_W^2}B_1\right)<y_Z<\beta_2^{TT}+\frac{1-\beta_W^2}{2\beta_W^2}B_2, \tag{33}$$

where $B_1=\beta_1^{LL}+\beta_1^{TT}+\beta_2^{TL}$ and $B_2=\beta_2^{LL}+\beta_2^{TT}+\beta_1^{TL}$. Adding these constraints to those in Eqs. (25) and (29) for x_γ and y_γ, we finally obtain separate bounds for the five anomalous couplings that determine the general expansion of Eq. (9). In this regard, we should notice the simplicity of this procedure to determine separate constraints on the trilinear couplings.

Actually, in addition to Eq. (29) there is one more condition on y_γ from the combination of Eqs. (25) and (27):

$$-(\alpha_1^{TL}+\alpha_2^{LL})<y_\gamma<\alpha_1^{LL}+\alpha_2^{TL}. \tag{34}$$

Numerically, which of the two is the most restrictive one depends on the value of the center of mass energy: indeed, it turns out that for $\sqrt{s}=500$ GeV the most stringent bound on y_γ is determined by Eq. (34), while Eq. (29) gives the most restrictive condition for 1 TeV.

The numerical results from these relations, and the chosen inputs for the luminosity and the initial polarization quoted previously, are summarized in Table II.

In a previous, model-independent, analysis of CP-conserving anomalous couplings [35], instead of the binning procedure followed here we used polarized cross sections integrated in angular ranges appropriately chosen in order to optimize the sensitivity to these parameters. Numerically, the results are qualitatively comparable, but the binning procedure leads to constraints improved by 10–50%, depending on the particular case.[3]

It should be interesting to specialize the procedure outlined above to the discussion of few model examples for nonstandard anomalous trilinear gauge boson couplings, where the number of such parameters is decreased. A popular framework is that in which anomalous values of the couplings reflect some new interaction effective at a mass scale Λ much higher than the Fermi scale. Correspondingly, at our (lower) energy scales, such effects represent corrections to the SM suppressed by inverse powers of Λ. As a natural requirement, given the observed phenomenological success of SU(2)×U(1), such a gauge symmetry (spontaneously broken and with γ, W, and Z the corresponding gauge bosons) is imposed also on the new interactions[4] [2]. The weak interaction is then described by an effective Lagrangian of the form

$$\mathscr{L}_W=\mathscr{L}_{\rm SM}+\sum_d\sum_k\frac{f_k^{(d)}}{\Lambda^{d-4}}\mathscr{O}_k^{(d)}, \tag{35}$$

where $\mathscr{L}_{\rm SM}$ is the SM interaction and the second term is the source of anomalous trilinear gauge boson couplings. This term takes the form of an expansion in inverse powers of Λ, where $\mathscr{O}_k^{(d)}$ are dimension d gauge invariant operators made of γ, W, Z and Higgs fields, and $f_k^{(d)}$ are coupling constants, not fixed by the symmetry. From the good agreement of the measured lepton couplings with the SM ones,

[3]The possibility to derive a separate bound by a similar analysis also on the anapole coupling z_Z (in the notation of Ref. [21]), which violates both C and P but conserves CP, was previously considered in Ref. [35]. CP-odd anomalous $WW\gamma$ couplings are independently (and stringently) constrained by the limit on the neutron electric dipole moment [36].

[4]Alternatives to imposing this symmetry have also been considered, see, e.g., Ref. [37].

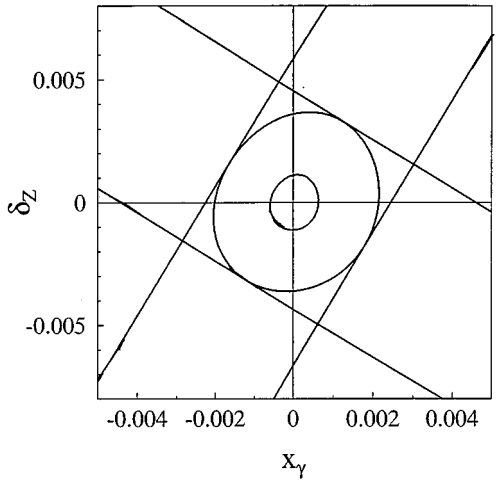

FIG. 5. Allowed domains (95% C.L.) for (x_γ, δ_Z) for the models with three [2] and two [40] independent couplings from $e^+e^- \to W_L^+ W_L^-$ with polarized electrons at $\sqrt{s}=0.5$ TeV and $\sqrt{s}=1$ TeV.

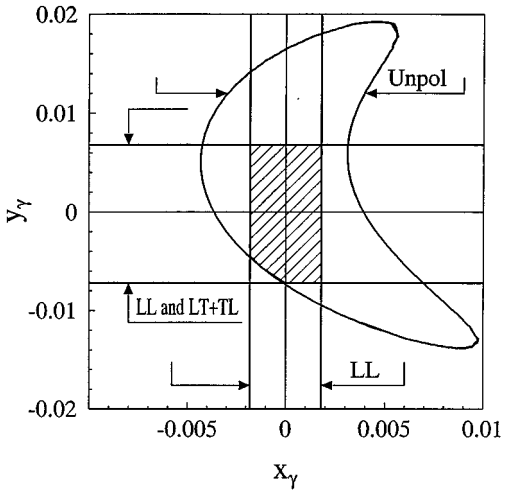

FIG. 6. Allowed domains (95% C.L.) for (x_γ, y_γ) for the models with two independent couplings (HISZ scenario [2]) from σ^L of process $e^+e^- \to W_L^+ W_L^-$ at $\sqrt{s}=0.5$ TeV. The notation ''unpol'' refers to unpolarized $W^\pm$ final states.

one assumes that such couplings remain unaffected by the new physics. Truncation of the sum in Eq. (35) to the lowest significant dimension, $d=6$, limits the number of allowed independent operators (and their corresponding constants) to three [2,4,38,39]:

$$\mathcal{O}_{WWW}^{(6)} = \mathrm{Tr}[\hat{W}_{\mu\nu}\hat{W}^{\nu\rho}\hat{W}_\rho^\mu],$$

$$\mathcal{O}_W^{(6)} = (D_\mu\Phi)^\dagger \hat{W}^{\mu\nu}(D_\nu\Phi),$$

$$\mathcal{O}_B^{(6)} = (D_\mu\Phi)^\dagger \hat{B}^{\mu\nu}(D_\nu\Phi). \tag{36}$$

Here, Φ is the Higgs doublet and, in terms of the B and W field strengths: $\hat{B}^{\mu\nu} = i(g'/2)B^{\mu\nu}$, $\hat{W}^{\mu\nu} = i(g/2)\vec{\tau}\cdot\vec{W}^{\mu\nu}$ with $\vec{\tau}$ the Pauli matrices. Therefore, in such a model, only three anomalous couplings are independent:

$$x_\gamma = \cos^2\theta_W (f_B^{(6)} + f_W^{(6)})\frac{M_Z^2}{2\Lambda^2}, \quad y_\gamma = f_{WWW}^{(6)}\frac{3M_W^2 g^2}{2\Lambda^2}, \tag{37}$$

$$\delta_Z = \cot\theta_W f_W^{(6)}\frac{M_Z^2}{2\Lambda^2}, \quad x_Z = -\tan\theta_W x_\gamma, \quad y_Z = \cot\theta_W y_\gamma. \tag{38}$$

According to Eqs. (37) and (38), in this model there are only three independent couplings which can be chosen to be x_γ, y_γ, and δ_Z. As mentioned in Ref. [2], the correlations between different anomalous trilinear gauge-boson couplings exhibited in Eqs. (37) and (38) are due to the truncation of the effective Lagrangian (35) at the dimension-six level, and do not hold any longer when dimension-eight (or higher) operators are included.

TABLE III. Limits on anomalous gauge boson couplings at the 95% C.L. for the models with three, two, and one independent parameters.

Model with three independent anomalous constants [2]: x_γ, y_γ, δ_Z, $x_Z=-\tan\theta_W x_\gamma$, $y_Z=\cot\theta_W y_\gamma$					
$\sqrt{s}$(TeV)	$x_\gamma(10^{-3})$	$\delta_Z(10^{-3})$	$x_Z(10^{-3})$	$y_\gamma(10^{-3})$	$y_Z(10^{-3})$
0.5	$-2.0-2.2$	$-3.8-3.8$	$-1.2-1.1$	$-7.0-7.5$	$-12.8-13.7$
1	$-0.6-0.6$	$-1.1-1.1$	$-0.3-0.3$	$-4.0-4.5$	$-7.3-8.2$
Model with two independent anomalous constants [2]: x_γ, y_γ, $\delta_Z=x_\gamma/2\sin\theta_W\cos\theta_W$, $x_Z=-\tan\theta_W x_\gamma$, $y_Z=\cot\theta_W y_\gamma$					
$\sqrt{s}$(TeV)	$x_\gamma(10^{-3})$	$\delta_Z(10^{-3})$	$x_Z(10^{-3})$	$y_\gamma(10^{-3})$	$y_Z(10^{-3})$
0.5	$-1.8-1.8$	$-2.1-2.1$	$-1.0-1.0$	$-6.6-6.8$	$-12.1-12.4$
1	$-0.5-0.5$	$-0.6-0.6$	$-0.3-0.3$	$-3.0-2.4$	$-5.5-4.4$
Model with one independent anomalous constant [41]: x_γ, $x_Z=-\tan\theta_W\, x_\gamma=-\sin^2\theta_W\delta_Z$					
$\sqrt{s}$(TeV)	$x_\gamma(10^{-3})$	$\delta_Z(10^{-3})$	$x_Z(10^{-3})$	y_γ	y_Z
0.5	$-1.1-1.1$	$-2.6-2.6$	$-0.6-0.6$	0	0
1	$-0.3-0.3$	$-0.8-0.8$	$-0.2-0.2$	0	0

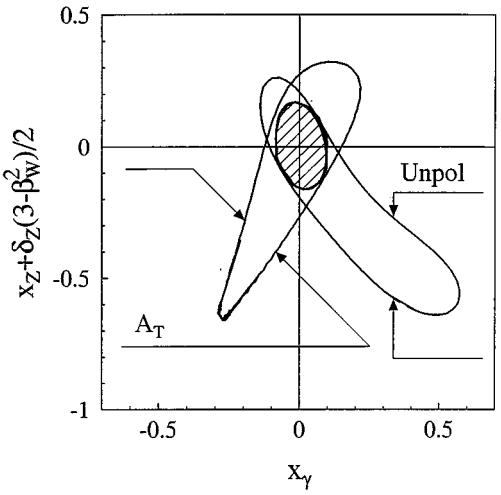

FIG. 7. Allowed domains (95% C.L.) for $[x_\gamma, x_Z+\delta_Z(3-\beta_W^2)/2]$ from $e^+e^-\to W_L^+W_L^-$ with unpolarized ($\sigma^{\rm unpol}$) and transversely polarized (A_T) initial e^+e^- beams at $\sqrt{s}=200$ GeV, inputs as specified in the text. The hatched allowed area: combination of $\sigma^{\rm unpol}$ and A_T.

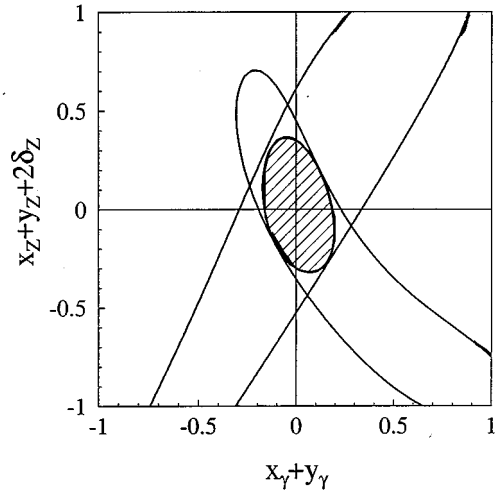

FIG. 8. Same as Fig. 7, for $(x_\gamma+y_\gamma, x_Z+y_Z+2\delta_Z)$ from $e^+e^-\to W_L^+W_T^-+W_T^+W_L^-$.

Further reduction in the number of the anomalous couplings occurs in the "Hagiwara-Ishihara-Szalapski-Zeppenfeld (HISZ) scenario" [2], where the relation $f_B^{(6)}=f_W^{(6)}$ in Eqs. (37) and (38) is assumed. In this case, the WWZ couplings are so related:

$$\delta_Z=\frac{1}{2\,\sin\theta_W\cos\theta_W}x_\gamma, \quad x_Z=-\tan\theta_W x_\gamma, \quad y_Z=\cot\theta_W y_\gamma. \tag{39}$$

Another way to reduce the number of independent trilinear anomalous couplings starts from imposing just global $SU(2)_L$ symmetry on the Lagrangian in Eq. (9). This directly implies the relation $x_Z=-\tan\theta_W x_\gamma$, the same as in Eq. (38). Further reduction is obtained by neglecting dimension-six quadrupole operators, so that $y_\gamma=y_Z=0$, and by cancelling the order s^2 tree-level unitarity violating contributions to WW scattering, which in turn leads to the condition $\delta_Z=x_\gamma/\sin\theta_W\cos\theta_W$ [40,41].

For the model with three parameters, the region allowed to (x_γ,δ_Z), presented in Fig. 5, corresponds to W_LW_L production, combining both left-handed and right-handed initial polarization. Comparing to the results in Table II, we notice that δ_Z can be more tightly constrained in this case than in the general one. Concerning the third independent coupling, y_γ, the best bounds are obtained from the combination of W_LW_L and W_LW_T production channels. In the case of the two-parameter model of Ref. [40], the bounds on x_γ and δ_Z are obtained in the same way as above, and are numerically identical.

The bounds relevant to the two-parameter model of Ref. [2] are shown in Fig. 6. In this case, due to relation (39) among the couplings, σ^L numerically proves to be more sensitive than σ^R. Concerning final state polarizations, the bound on x_γ is obtained from W_LW_L production, while that on y_γ involves the combination of both LL and $TL+LT$ polarized cross sections. For an illustration, in Fig. 6 we also report the region allowed by the cross section for unpolarized W's.

Table III summarizes the numerical bounds that can be obtained from our analysis for the models of anomalous couplings considered here.

V. BOUNDS ON ANOMALOUS COUPLINGS FROM LEP 200

At this facility, no initial beam longitudinal polarization is planned [42]. As anticipated in Sec. I, to perform a model-independent analysis of all five CP-even couplings following the procedure above, $\sigma^{\rm unpol}$ can play the role of σ^L (having a similar dependence on these couplings), and the azimuthal asymmetry A_T in Eq. (17) can be combined with $\sigma^{\rm unpol}$ to give the bounds. Thus, we assume that the transverse polarization of initial beams will be available, and that the final W's polarizations could be measured with the same

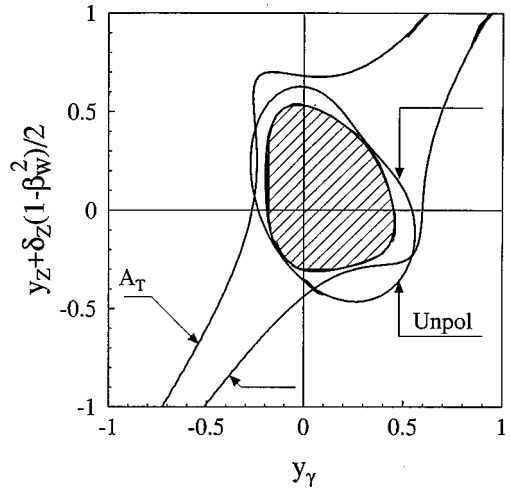

FIG. 9. Same as Fig. 7, for $[y_\gamma, y_Z+\delta_Z(1-\beta_W^2)/2]$ from $e^+e^-\to W_T^+W_T^-$.

TABLE IV. Model-independent limits on the five CP-even nonstandard gauge boson couplings at the 95% C.L. for LEP 200.

$\sqrt{s}$(GeV)	$x_\gamma(10^{-1})$	$y_\gamma(10^{-1})$	$\delta_Z(10^{-1})$	$x_Z(10^{-1})$	$y_Z(10^{-1})$
200	$-0.9-1.0$	$-2.0-2.9$	$-26.4-23.6$	$-32.8-36.7$	$-10.6-13.1$
230	$-0.5-0.6$	$-1.4-2.0$	$-15.6-13.8$	$-18.5-20.8$	$-5.7-7.6$

efficiency used in the previous sections. Due to the limited statistics provided by the luminosity at LEP 200:

$$\int Ldt = 500 \text{ pb}^{-1} \text{ (LEP 200)}, \tag{40}$$

we take six equal bins in order to have a significant number of events per beam and, furthermore, we assume the same systematic uncertainty as in Eq. (24) as well as the same reconstruction efficiency ε_W. By performing the same kind of analysis presented in the previous section, we would find for the combinations of anomalous couplings relevant to Eqs. (18)–(20) the 95% C.L. allowed regions presented in Figs. 7–9, respectively. These are the analogues of Figs. 2–4 for the case of NLC. Quite similarly, the constraints at LEP correspond to the combinations of the bounds from A_T and σ^{unpol} for W_LW_L, $W_LW_T+W_TW_L$, and W_TW_T production, respectively. In the last case, from Fig. 9 one can notice that the azimuthal asymmetry is not so helpful to minimize the combined allowed region, which therefore in almost entirely determined by σ^{unpol}.

By combining the analogues of Eqs. (25)–(34), one can disentangle the bounds for the different couplings constants. The numerical results are presented in Table IV for two values of the c.m. energy, namely $\sqrt{s}=200$ and 230 GeV, and the luminosity in Eq. (40). As expected, the constraints become more stringent with increasing energy.

Concerning the application of this approach to models with a reduced number of independent anomalous couplings, the expected sensitivities, for the same model examples considered in the previous section, are exposed in Table V.

VI. CONCLUDING REMARKS

One of the basic points of the analysis presented above is the use of final $W^\pm$ polarization to group the five independent anomalous trilinear gauge boson couplings into pairs of ''effective'' combinations as in Eqs. (18)–(20), *via* the specific dependence of the helicity amplitudes relevant to the considered differential cross sections. Such cross sections for polarized W's should be obtained experimentally from angular distributions of the $W^\pm$ decay products [8]. This leads to a simplified two-dimensional analysis (rather than a three- or a five-dimensional one) for each final polarization and, by a χ^2 procedure, bounds in the two-parameter planes of the corresponding pairs of ''effective'' coupling constants are obtained.

The initial electron beam polarization (either longitudinal or transverse) turns out to have a fundamental role in drastically reducing the above-mentioned two-dimensional allowed regions. Finally, by combining Eqs. (25)–(30), one can obtain separate bounds for each of the five CP-even couplings. Thus in summary, while the specific dependence of the final state polarization on the anomalous couplings allows a model-independent analysis of the general case, initial beam polarization can be used to further restrict the bounds.

From the numerical point of view, the bounds presented in

TABLE V. Limits on anomalous gauge boson couplings at the 95% C.L. for the models with three, two, and one independent parameters for LEP 200.

Model with three independent anomalous constants [2]: x_γ, y_γ, δ_Z, $x_Z=-\tan\theta_W x_\gamma$, $y_Z=\cot\theta_W y_\gamma$					
$\sqrt{s}$(GeV)	$x_\gamma(10^{-1})$	$\delta_Z(10^{-1})$	$x_Z(10^{-1})$	$y_\gamma(10^{-1})$	$y_Z(10^{-1})$
200	$-0.86-0.94$	$-1.2-1.3$	$-0.51-0.47$	$-1.4-2.2$	$-2.56-4.02$
230	$-0.52-0.62$	$-1.0-1.1$	$-0.34-0.28$	$-1.0-2.0$	$-1.8-3.66$
Model with two independent anomalous constants [2]: x_γ, y_γ, $\delta_Z=x_\gamma/2\sin\theta_W\cos\theta_W$, $x_Z=-\tan\theta_W x_\gamma$, $y_Z=\cot\theta_W y_\gamma$					
$\sqrt{s}$(GeV)	$x_\gamma(10^{-1})$	$\delta_Z(10^{-1})$	$x_Z(10^{-1})$	$y_\gamma(10^{-1})$	$y_Z(10^{-1})$
200	$-0.6-0.7$	$-0.71-0.83$	$-0.38-0.33$	$-1.5-1.5$	$-2.7-2.2$
230	$-0.42-0.48$	$-0.5-0.57$	$-0.26-0.23$	$-1.1-1.2$	$-2.0-2.2$
Model with one independent anomalous constant [41]: x_γ, $x_Z=-\tan\theta_W\, x_\gamma=-\sin^2\theta_W\, \delta_Z$					
$\sqrt{s}$(GeV)	$x_\gamma(10^{-1})$	$\delta_Z(10^{-1})$	$x_Z(10^{-1})$	y_γ	y_Z
200	$-0.39-0.41$	$-0.93-0.97$	$-0.22-0.21$	0	0
230	$-0.30-0.33$	$-0.71-0.78$	$-0.18-0.16$	0	0

Tables II–V are rather stringent and clearly, for a more complete test of the SM, the electroweak corrections [20] can be included in the analysis. Furthermore, the sensitivity to anomalous couplings indicated by these results crucially depends on the chosen inputs, in particular on the assumed value of the polarized $W^{\pm}$ reconstruction efficiency, so that the analysis needs to be supplemented by a more detailed knowledge of the experimental performances.

Finally, we recall that the procedure presented here is based on the differential W^+W^- production cross section. However, looking for further increased sensitivity to the anomalous couplings, it might be worthwhile to apply a similar analysis to more detailed observables including angular distributions of W^+ and W^- decay products, such as those considered in Refs. [8,9], and try to assess there the distinguished role of initial e^+e^- polarization.

ACKNOWLEDGMENTS

Two of us (V.V.A. and A.A.P.) acknowledge the support and the hospitality of INFN-Sezione di Trieste and of the International Centre for Theoretical Physics, Trieste. They also acknowledge the support from the International Science Foundation and Belarussian Government, Grant No. F9D100. N.P. was also supported by the Italian Ministry of University, Scientific Research and Technology (MURST).

APPENDIX

The integrated cross section of process (1) defined in Eq. (22) can be generally expressed, for arbitrary degrees of longitudinal polarization of electrons (P_L) and positrons ($\tilde{P}_L$), as ($z \equiv \cos\theta$)

$$\sigma(z_1,z_2)=\frac{1}{4}[(1+P_L)\cdot(1-\tilde{P}_L)\sigma^+(z_1,z_2) + (1-P_L)\cdot(1+\tilde{P}_L)\sigma^-(z_1,z_2)]. \quad \text{(A1)}$$

The corresponding integrated cross sections for polarized final W's, to be inserted in Eq. (A1), can be written as

$$\sigma^{+,-}_{\alpha\beta}(z_1,z_2)=C\sum_{i=0}^{i=11} F_i^{+,-}\mathcal{O}_{i,\alpha\beta}(z_1,z_2), \quad \text{(A2)}$$

where $C=\pi\alpha^2_{\rm em}\beta_W/2s$, the helicities of the initial e^+e^- and final W^+W^- states are labeled as $+,-$ ($\lambda=-\lambda'=\pm 1/2$) and $\alpha\beta=(LL,TT,TL)$, respectively. In Eq. (A2) we use the following notation: $\mathcal{O}_{i,\alpha\beta}(z_1,z_2)\equiv\mathcal{O}_{i,\alpha\beta}(z_2)-\mathcal{O}_{i,\alpha\beta}(z_1)$, where $\mathcal{O}_{i,\alpha\beta}$ are functions of the kinematical variables which characterize the various possibilities for the final W^+W^- polarizations (or the sum over all polarizations for unpolarized W's). The F_i are combinations of coupling constants, where the anomalous trilinear gauge boson couplings explicitly appear. For the case of right-handed electrons (and left-handed positrons) we have, with χ_Z the Z boson propagator:

$$F_1^+=2(1-g_Zg_e^R\cdot\chi_Z)^2,$$

$$F_3^+=x_\gamma-g_e^R(x_Z+x_\gamma g_Z)\cdot\chi_Z+(g_e^R\cdot\chi_Z)^2g_Zx_Z,$$

$$F_4^+=y_\gamma-g_e^R(y_Z+y_\gamma g_Z)\cdot\chi_Z+(g_e^R\cdot\chi_Z)^2g_Zy_Z,$$

$$F_9^+=\frac{1}{2}(x_\gamma-g_e^Rx_Z\cdot\chi_Z)^2,\quad F_{10}^+=\frac{1}{2}(y_\gamma-g_e^Ry_Z\cdot\chi_Z)^2,$$

$$F_{11}^+=\frac{1}{2}[x_\gamma y_\gamma-g_e^R(x_\gamma y_Z+x_Zy_\gamma)\cdot\chi_Z+(g_e^R\cdot\chi_Z)^2x_Zy_Z]. \quad \text{(A3)}$$

The remaining F^+ are zero. For the case of left-handed electrons (and right-handed positrons),

$$F_0^-=\frac{1}{16s_W^4},\quad F_1^-=2(1-g_Zg_e^L\cdot\chi_Z)^2,$$

$$F_2^-=-\frac{1}{2s_W^2}(1-g_Zg_e^L\cdot\chi_Z),$$

$$F_3^-=x_\gamma-g_e^L(x_Z+x_\gamma g_Z)\cdot\chi_Z+(g_e^L\cdot\chi_Z)^2g_Zx_Z,$$

$$F_4^-=y_\gamma-g_e^L(y_Z+y_\gamma g_Z)\cdot\chi_Z+(g_e^L\cdot\chi_Z)^2g_Zy_Z,$$

$$F_6^-=-\frac{1}{4s_W^2}(x_\gamma-x_Zg_e^L\cdot\chi_Z),$$

$$F_7^-=-\frac{1}{4s_W^2}(y_\gamma-y_Zg_e^L\cdot\chi_Z),$$

$$F_9^-=\frac{1}{2}(x_\gamma-g_e^Lx_Z\cdot\chi_Z)^2,$$

$$F_{10}^-=\frac{1}{2}(y_\gamma-g_e^Ly_Z\cdot\chi_Z)^2,$$

$$F_{11}^-=\frac{1}{2}[x_\gamma y_\gamma-g_e^L(x_\gamma y_Z+x_Zy_\gamma)\cdot\chi_Z+(g_e^L\cdot\chi_Z)^2x_Zy_Z]. \quad \text{(A4)}$$

The remaining F^- are zero. Equations (A3) and (A4) are obtained in the approximation where the imaginary part of the Z boson propagator is neglected. Accounting for this effect requires the replacements $\chi\to{\rm Re}\chi$ and $\chi^2\to|\chi|^2$ in the right-hand sides of Eqs. (A3) and (A4).

In Eq. (A2), for the longitudinal (LL) cross sections $\sigma(e^+e^-\to W_L^+W_L^-)$,

$$\mathcal{O}_{0,LL}(z)=\frac{s}{4M_W^4}[s^3(J_0-J_4)-4M_W^4(3s+4M_W^2)(J_0-J_2) -4(s+2M_W^2)|\vec{p}|s\sqrt{s}(J_1-J_3)],$$

$$\mathcal{O}_{1,LL}(z)=\frac{s^3-12sM_W^4-16M_W^6}{8sM_W^4}K_1,$$

$$\mathcal{O}_{2,LL}(z)=\frac{|\vec{p}|s\sqrt{s}(s+2M_W^2)}{2M_W^4}(I_1-I_3) -\frac{s^3-12sM_W^4-16M_W^6}{4M_W^4}(I_0-I_2),$$

$$\mathcal{O}_{3,LL}(z)=\frac{s^2-2M_W^2 s-8M_W^4}{2M_W^4}K_1,$$

$$\mathcal{O}_{4,LL}(z)=\mathcal{O}_{5,LL}(z)=\mathcal{O}_{7,LL}(z)=\mathcal{O}_{8,LL}(z)=\mathcal{O}_{10,LL}(z)=\mathcal{O}_{11,LL}(z)=0,$$

$$\mathcal{O}_{6,LL}(z)=\frac{s}{2M_W^4}[(8M_W^4+2sM_W^2-s^2)(I_0-I_2)+2s|\vec{p}|\sqrt{s}(I_1-I_3)],$$

$$\mathcal{O}_{9,LL}(z)=2\frac{s|\vec{p}|^2}{M_W^4}K_1. \tag{A5}$$

For the transverse (TT) cross sections $\sigma(e^+e^-\to W_T^+W_T^-)$,

$$\mathcal{O}_{0,TT}(z)=4s[s(J_0-J_4)-2M_W^2(J_0-J_2)-2|\vec{p}|\sqrt{s}(J_1-J_3)],$$

$$\mathcal{O}_{1,TT}(z)=\frac{M_W^2}{2s}\mathcal{O}_{4,TT}(z)=\frac{M_W^4}{s^2}\mathcal{O}_{10,TT}(z)=\frac{4|\vec{p}|^2}{s}K_1,$$

$$\mathcal{O}_{2,TT}(z)=\frac{M_W^2}{s}\mathcal{O}_{7,TT}(z)=4|\vec{p}|\sqrt{s}(I_1-I_3)-8|\vec{p}|^2(I_0-I_2),$$

$$\mathcal{O}_{3,TT}(z)=\mathcal{O}_{5,TT}(z)=\mathcal{O}_{6,TT}(z)=\mathcal{O}_{8,TT}(z)=\mathcal{O}_{9,TT}(z)=\mathcal{O}_{11,TT}(z)=0. \tag{A6}$$

Finally, for the production of one longitudinal plus one transverse vector boson ($TL+LT$),

$$\mathcal{O}_{0,TL}(z)=\frac{2s}{M_W^2}[s^2(J_0+J_4)-4|\vec{p}|\sqrt{s}(4|\vec{p}|^2J_1+sJ_3)+4M_W^4(J_0+J_2)+2s(s-6M_W^2)J_2-4sM_W^2J_0], \tag{A7}$$

$$2\mathcal{O}_{1,TL}(z)=\mathcal{O}_{3,TL}(z)=\mathcal{O}_{4,TL}(z)=\mathcal{O}_{11,TL}(z)=2\mathcal{O}_{9,TL}(z)=2\mathcal{O}_{10,TL}(z)=\frac{8|\vec{p}|^2}{M_W^2}K_2,$$

$$\mathcal{O}_{2,TL}(z)=\mathcal{O}_{6,TL}(z)=\mathcal{O}_{7,TL}(z)=\frac{4|\vec{p}|\sqrt{s}}{M_W^2}[4|\vec{p}|^2I_1+sI_3-2|\vec{p}|\sqrt{s}(I_0+I_2)],$$

$$\mathcal{O}_{5,TL}(z)=\frac{16|\vec{p}|^3\sqrt{s}z^2}{M_W^4},$$

$$\mathcal{O}_{8,TL}(z)=\frac{16s|\vec{p}|^2}{M_W^4}[M_W^2I_0+2|\vec{p}|\sqrt{s}I_1-(s-M_W^2)I_2].$$

In Eqs. (A5)–(A7) the functions I, J, and K are ($d=M_W^2-s/2$, $b=s\beta_W^2/2$, $t=d+bz$):

$$I_0(z)=\frac{1}{b}\ln|t|,$$

$$I_1(z)=\frac{1}{b^2}(t-d\,\ln|t|),$$

$$I_2(z)=\frac{1}{b^3}\left(\frac{t^2}{2}-2dt+d^2\ln|t|\right),$$

$$I_3(z)=\frac{1}{b^4}\left(\frac{t^3}{3}-\frac{3dt^2}{2}+3d^2t-d^3\ln|t|\right),$$

$$J_0(z)=-\frac{1}{bt},$$

$$J_1(z)=\frac{1}{b^2}\left(\ln|t|+\frac{d}{t}\right),$$

$$J_2(z)=\frac{1}{b^3}\left(t-2d\ln|t|-\frac{d^2}{t}\right),$$

$$J_3(z)=\frac{1}{b^4}\left(\frac{t^2}{2}-3dt+3d^2\ln|t|+\frac{d^3}{t}\right),$$

$$J_4(z)=\frac{1}{b^5}\left(\frac{t^3}{3}-\frac{4dt^2}{2}+6d^2t-4d^3\ln|t|-\frac{d^4}{t}\right),$$

$$K_{1,2}(z)=z\mp\frac{z^3}{3}. \tag{A8}$$

[1] *Precision Tests of the Standard Electroweak Model*, edited by P. Langacker, Advanced Series on Directions in High Energy Physics, Vol. 14 (World Scientific, Singapore, 1995).

[2] K. Hagiwara, S. Ishihara, R. Szalapski, and D. Zeppenfeld, Phys. Lett. B **283**, 353 (1992); Phys. Rev. D **48**, 2182 (1993).

[3] P. Hernández and F.J. Vegas, Phys. Lett. B **307**, 116 (1993).

[4] A. De Rujula, M.B. Gavela, P. Hernandez, and E. Massó, Nucl. Phys. **B384**, 3 (1992).

[5] F. Abe *et al.*, Phys. Rev. Lett. **74**, 1936 (1995); **74**, 1941 (1995); **75**, 1017 (1995); S. Abachi *et al.*, *ibid.* **75**, 1023 (1995).

[6] K. Hagiwara, R.D. Peccei, D. Zeppenfeld, and K. Hikasa, Nucl. Phys. **B282**, 253 (1987).

[7] G.L. Kane, J. Vidal, and C.-P. Yuan, Phys. Rev. D **39**, 2617 (1989).

[8] M. Bilenky, J.L. Kneur, F.M. Renard, and D. Schildknecht, Nucl. Phys. **B409**, 22 (1993).

[9] R.L. Sekulin, Phys. Lett. B **338**, 369 (1994).

[10] U. Baur and D. Zeppenfeld, Nucl. Phys. **B325**, 253 (1989); P. Salati and J.C. Wallet, Z. Phys. C **16**, 155 (1982); G. Altarelli, G. Martinelli, B. Mele, and R. Ruckl, Nucl. Phys. **B262**, 204 (1985); M. Böhm and A. Rosado, Z. Phys. C **39**, 275 (1988).

[11] U. Baur and D. Zeppenfeld, Nucl. Phys. **B308**, 127 (1988); D. Zeppenfeld and S. Willenbrock, Phys. Rev. D **37**, 1775 (1988); U. Baur and D. Zeppenfeld, Phys. Lett. B **201**, 383 (1988); U. Baur and E.L. Berger, Phys. Rev. D **41**, 1476 (1990); E.N. Argyres, F. Diakonos, O. Korakianitis, C. G. Papadopoulos, and W. J. Stirling, Phys. Lett. B **272**, 431 (1991).

[12] U. Baur, J. Ohnemus, and T. Han, Phys. Rev. D **51**, 3381 (1995).

[13] M. Bilenky, J.L. Kneur, F.M. Renard, and D. Schildknecht, Nucl. Phys. **B419**, 240 (1994); T. Barklow, in *Physics and Experiments with Linear Colliders*, Proceedings of the Workshop Saariselka, Finland, 1991, edited by R. Orava, P. Eerola, and M. Nordberg (World Scientific, Singapore, 1992), Vol. I, p. 423.

[14] P. Sushkov, V.V. Flambaum, and I.B. Khriplovich, Sov. J. Nucl. Phys. **20**, 537 (1975); W. Alles, Ch. Boyer, and A.J. Buras, Nucl. Phys. **B119**, 125 (1977); R.W. Brown and K.O. Michaelian, Phys. Rev. D **19**, 922 (1979).

[15] A.A. Pankov and N. Paver, Phys. Lett. B **274**, 483 (1992); Phys. Rev. D **48**, 63 (1993).

[16] A.A. Babich, A.A. Pankov, and N. Paver, Phys. Lett. B **299**, 351 (1993); **346**, 303 (1995).

[17] A. Blondel *et al.*, in *Proceedings of the ECFA Workshop on LEP 200*, Aachen, 1986, edited by A. Böhm and W. Hoogland CERN Report No. 87-08 (Geneva, Switzerland, 1987), Vol. I, p. 120.

[18] M. Frank, P. Mättig, R. Settles, and W. Zeuner, in *Proceedings of the Workshop, e^+e^- Collisions at 500 GeV: The Physics Potential*, Munich-Annecy-Hamburg, 1991, edited by P.M. Zerwas (DESY Report No. 92-123B, Hamburg, 1992), p. 223.

[19] D. Zeppenfeld, Phys. Lett. B **183**, 380 (1987).

[20] J. Fleischer, K. Kolodziej, and F. Jegerlehner, Phys. Rev. D **49**, 2174 (1994).

[21] G. Gounaris, J.L. Kneur, J. Layssac, G. Moultaka, F.M. Renard, and D. Schildknecht, in *Proceedings of the Workshop e^+e^- Collisions at 500 GeV: The Physics Potential* [18], p. 735.

[22] W.A. Bardeen, R. Gastmans, and B. Lautrup, Nucl. Phys. **B46**, 319 (1982); K.J. Kim and Y.S. Tsai, Phys. Rev. D **12**, 3972 (1975).

[23] G. Couture and J.N. Ng, Z. Phys. C **35**, 65 (1987).

[24] G. Couture, J.N. Ng, J.L. Hewett, and T.G. Rizzo, Phys. Rev. D **38**, 860 (1988).

[25] A.B. Lahanas and V.C. Spanos, Phys. Lett. B **334**, 378 (1994); Z. Phys. C **65**, 544 (1995); A. Culatti, *ibid.* **65**, 537 (1995).

[26] C.P. Burgess, S. Godfrey, H. König, D. London, and I. Maksymyk, Phys. Rev. D **49**, 6115 (1994).

[27] H. Aihara *et al.*, "Summary of the DPF Working Subgroup on Anomalous Gauge Boson Interactions of the DPF Long Range Planning Study," in *Electroweak Symmetry Breaking and Beyond the Standard Model*, edited by T. Barklow, S. Dawson, H. Haber, and J. Seigrist, Fermilab Report No. FERMILAB-Pub-95-031, 1995 (unpublished).

[28] C.Y. Prescott, in *Proceedings of the Workshop* on *Physics and Experiments with Linear e^+e^- Colliders*, Waikoloa, Hawaii, 1993, edited by F.A. Harris, S.L. Olsen, S. Pakvasa, and X. Tata (World Scientific, Singapore, 1993), p. 379.

[29] R.W. Forty, J.B. Hansen, J.D. Hansen, and R. Settles, *Collisions at 500 GeV: the Physics Potential*, edited by P.M. Zerwas (DESY Report No. DESY 93-123C, 1993), p. 235.

[30] R. Settles, *Collisions at 500 GeV* [29], p. 591.

[31] H. Anlauf, A. Himmler, P. Manakos, T. Mannel, and H. Dahmen, in *Proceedings of the Workshop on Physics and Experiments with Linear e^+e^- Colliders* [28], p. 708.

[32] D. L. Hartill *et al.*, "Reports of the Working Group on Accelerator Physics, Technologies and Facilities of the DPF Long Term Planning Study," SLAC Report No. SLAC-PUB-6751, 1995 (unpublished).

[33] Review of Particle Properties, Phys. Rev. D **50**, 1271 (1994).

[34] F. Cuypers, Max Planck Institute Report No. MPI-PhT-95-16, 1995 (unpublished).

[35] A.A. Pankov and N. Paver, Phys. Lett. B **324**, 224 (1994); **346**, 115 (1995).

[36] F. Boudjema, K. Hagiwara, C. Hamzaoui, and K. Numata, Phys. Rev. D **43**, 2223 (1991).

[37] J.-M. Frére, J.M. Moreno, J. Orloff, and M. Tytgat, Nucl. Phys. **B429**, 3 (1994).

[38] W. Buchmüller and D. Wyler, Nucl. Phys. **B268**, 621 (1986).

[39] G. Gounaris and F.M. Renard, Z. Phys. C **59**, 133 (1993).

[40] M. Kuroda, J. Maalampi, K.H. Schwarzer, and D. Schildknecht, Nucl. Phys. **B284**, 271 (1987).

[41] C. Bilchak, M. Kuroda, and D. Schildknecht, Nucl. Phys. **B299**, 7 (1988).

[42] D. Treille, in *Precision Tests of the Standard Electroweak Model* [1].